FEBS Letters 525 (2002) 100–104 FEBS 26352

Crystal structure of Rnd3/RhoE: functional implications[1]

Dennis Fiegen, Lars Blumenstein, Patricia Stege, Ingrid R. Vetter, Mohammad Reza Ahmadian*

Max-Planck-Institut für molekulare Physiologie, Abteilung Strukturelle Biologie, Otto-Hahn-Strasse 11, 44227 Dortmund, Germany

Received 30 April 2002; revised 3 July 2002; accepted 9 July 2002

First published online 19 July 2002

Edited by Irmgard Sinning

Abstract The Rnd proteins constitute an exceptional subfamily within the Rho GTPase family. They possess extended chains at both termini and four prominent amino acid deviations causing GTPase deficiency. Herein, we report the crystal structure of the Rnd3/RhoE G-domain (amino acids 19–200) at 2.0 Å resolution. This is the first GTP-structure of a Rho family member which reveals a similar fold but striking differences from RhoA concerning (i) GTPase center, (ii) charge distribution at several surface areas, (iii) C3-transferase binding site and (iv) interacting interfaces towards RhoA regulators and effectors.

Key words: Rnd3; RhoE; RhoA; Crystal structure; GTPase

1. Introduction

The guanine nucleotide-binding proteins of the Rho subfamily control a large variety of biological processes, many of which are associated with dynamic cytoskeletal reorganization [1]. These proteins act as molecular switches cycling between two conformational states, the inactive GDP-bound and the active GTP-bound state. The cycling rate is controlled by two biochemically different reactions, the GDP/GTP exchange and the GTP-hydrolysis (GTPase reaction). These intrinsically very slow reactions can be accelerated dramatically by guanine nucleotide exchange factors (GEFs) of the Dbl family and GTPase activating proteins (GAPs) [1,2]. The activated Rho proteins subsequently bind to their downstream effectors mediating the cellular response [3]. The signalling pathway is switched off via GAP-dependent stimulation of the GTP-hydrolysis reaction of the Rho proteins [2]. An additional level of regulation is provided by guanine nucleotide dissociation inhibitors (GDIs) that spatially dislodge the Rho proteins from their subcellular membrane localization [4].

Recently, the GTP-binding proteins of the Rnd subfamily (Rnd1/Rho6, Rnd2/Rho7 and Rnd3/RhoE/Rho8) have been described as novel and unusual members of the Rho family that display substantial structural differences compared to the classical molecular switches [5]: (i) they have a N-terminal (2–18 residues) and a C-terminal (about 30 residues) extension compared to Rho proteins; (ii) unlike most other Rho proteins that are geranylgeranylated, Rnd3 is farnesylated at the C-terminus (CAAX box). The CAAX box is required for proper membrane localization; (iii) most remarkably, these proteins harbor amino acid deviations at codons 12, 13, 59 and 61 (Ras numbering) [6]. Mutation of the respective codons in Ras genes are found in 40% of human tumors and are responsible for the Ras-mediated malignant transformation [7]. Impaired GTPase activity, particularly in the presence of RasGAPs, has been found to be the biochemical reason behind the oncogenicity of Ras [8]. Accordingly, Rnd proteins may exist merely in the GTP-bound conformation since they are unable to hydrolyze GTP and –in addition– resistant towards GAP activity [6,9,10].

It is currently believed that Rnd proteins antagonize some effects of the RhoA-induced cytoskeletal reorganization, due to the following observations: (i) transient expression of Rnd1 and Rnd3 inhibit the assembly of actin stress fibers and the formation of integrin-based focal adhesions in fibroblasts and MDCK cells, respectively [9,10]. These rearrangements of the actin cytoskeleton are regulated cooperatively by two RhoA downstream effectors, ROCK and mDia [11]; (ii) in MDCK cells, the activation of the RAF–MEK–ERK kinase cascade induces Rnd3 expression leading to loss of actin stress fibers [12]; (iii) contrary to the effect of RhoA activation, Rnd3 promotes scatter factor-stimulated MDCK cell migration [10]; (iv) *Xenopus* Rnd1 (XRnd1) disrupts cell adhesion in early embryogenesis which can be fully restored by a constitutively active RhoA mutant [13]. It is therefore implicated that Rnd proteins may interfere with the Rho activation or with RhoA downstream signalling by binding and sequestering either of these proteins [9,10].

Here, we present the crystal structure of the Rnd3 G-domain (amino acids 19–200) at high resolution (2.0 Å). A detailed comparison between the Rnd3 and RhoA structures provides insights into distinct structural differences implicating a different intermolecular specificity.

2. Materials, methods, molecular replacement and crystallographic refinement

The G-domain of Rnd3 (19–200) was isolated as glutathione *S*-transferase fusion protein and purified after cleavage with thrombin by size exclusion chromatography (Superdex G75, Pharmacia, Freiburg, Germany). The concentration of the bound nucleotide and GTP hydrolysis were analyzed by reversed-phase high-performance liquid chromatography as described [14]. Due to degradation of the full length protein the G-domain was chosen for crystallization.

Crystals were grown at 20°C using the hanging-drop method by mixing 2 μl of a 1 mM solution of the Rnd3 G-domain in 20 mM

*Corresponding author. Fax: (49)-231-1332199.
E-mail address: reza.ahmadian@mpi-dortmund.mpg.de (M.R. Ahmadian).

[1] The atomic coordinates and structure factors (code 1M7B) have been deposited in the Protein Data Bank

0014-5793/02/$22.00
PII: S0014-5793(02)03094-6

Table 1
Data collection and refinement statistics of Rnd3

Intensity data processing	
Resolution	2.0 Å
Number of measurements	48439
Number of independent reflections	14843
R_{sym}[a]	9.2 (32.5)[b]
Completeness	98.6 (98.2)[b]
Mean $\langle I/\sigma(I)\rangle$	8.4 (1.5)[b]
Molecular replacement statistics	
Resolution range rotation/translation	12.0–5.0 Å/8.0–4.0 Å
Rotation[c]	9.6, 73.17, 267.46
Translation[c]	−9.48, 35.39, 30.04
Correlation coefficient	59.8 (31.8)[d]
R_{cryst}[e]	39.0 (48.8)[d]
Refinement statistics	
R_{cryst}[e]	20.1
R_{free}[e]	24.3
R.m.s. bond lengths	0.006
R.m.s. bond angles	1.2

[a] $R_{sym} = 100 \cdot \Sigma |I - \langle I\rangle| / \Sigma I$.
[b] In parenthesis are quantities calculated in the highest resolution bin at 2.07–2.0 Å.
[c] Eulerian angles (α,β,γ) are as defined in AMoRe and translations in the orthogonal system.
[d] In parenthesis are quantities of the second-best solution.
[e] $R_{cryst} = 100 \cdot \Sigma |F_o - F_c| / \Sigma F_o$. R_{free} is R_{cryst} that was calculated using 10% of the data, chosen randomly, and omitted from the subsequent structure refinement.

Tris/HCl pH 7.5, 2 mM $MgCl_2$, 2 mM DTE with 2 μl reservoir solution consisting of 100 mM sodium acetate buffer pH 4.6 and 8% PEG4000. X-ray diffraction data was collected at room temperature with a MAR 345 Image Plate System detector (X-Ray Research GmbH, Norderstedt, Germany) using focused X-rays from a FR591 rotating-CuKα-anode generator (Enraf Nonius, Delft, The Netherlands) equipped with osmic mirrors (X-Ray Research GmbH, Norderstedt). Data reduction and processing were done using the DENZO/SCALEPACK program package [15] (Table 1). The crystal diffracted up to 2.0 Å resolution and belonged to space group I222 ($a = 63.592$, $b = 69.932$, $c = 97.715$), with one molecule in the asymmetric unit.

The structure of the GTP-bound Rnd3 G-domain was solved by molecular replacement with the program AMoRe (Table 1) [16]. For this purpose the RhoA(G14V)·GTPγS structure (PDB code 1A2B) was employed as a search model [17]. After 20 rounds of model building using the program O and simulated annealing refinement with CNS the crystallographic R value was 20.1% (free R value of 4.3%)[18,19]. The final model includes 179 residues of Rnd3, one GTP molecule, one magnesium ion and 48 water molecules. The N-terminal residues Gly-Ser-Asn-Gln-Asn (Gly-Ser due to the thrombin cleavage site) could not be observed in the electron density map. The residues 22–23 (Val–Lys) and 200 (Lys) are included as alanines in the model.

3. Results and discussion

3.1. Overall fold and nucleotide binding

A ribbon plot in Fig. 1 showing the secondary structure elements of the Rnd3 structure is superimposed onto the GTPγS-bound Rho(G14V) model [17]. The main features consisting of a six-stranded β-sheet (five parallel and one antiparallel) surrounded by five α-helices connected by loops and one insert helix are conserved, as found in Cdc42, Rac and RhoA proteins (Figs. 1 and 2A) [17,20–23]. The obvious minor differences between both structures correspond to the low root mean square deviation (r.m.s.d.) of 0.79 Å for 177 common Cα-atoms. A large number of polar and non-polar interactions dictating the guanine nucleotide binding in small GTPases are mostly conserved in Rnd3 too. However, the GTP-binding site of Rnd3 reveals two remarkable differences in the GTP coordination as compared to RhoA. The first difference is an additional water molecule in Rnd3 which contacts the invariant Ala179 of the ^{177}CSAL-motif and the carbonyl oxygen of the base. The second difference is the additional stabilization of the invariant Lys136 of the ^{135}CKSD-motif by Asp103 which is Ser85 in RhoA.

3.2. Defective GTPase center

It has been shown before by several groups that Rnd proteins are unable to hydrolyze GTP and –in addition– are resistant towards GAP activity [6,9,10]. The G-domain of Rnd3 is also completely disabled to hydrolyze GTP in the absence and in the presence of p50RhoGAP (data not shown). Four amino acid deviations are responsible for the Rnd3 GTPase deficiency: Ser32 (Gly14 in Rho), Gln33 (Ala15), Ser79 (Ala61) and Ser81 (Gln63) (Fig. 2A). Mutations of the respective codons in *ras* genes (Gly12, Gly13, Ala59 and Gln61), found in human tumors are responsible for Ras-mediated malignant transformation [7]. The structural status of the four deviating residues in Rnd3 are highlighted in Fig. 2B. The side chain of Ser81, which corresponds to the catalytically active Gln63 in RhoA, is rotated away from the γ-phosphate and is unable to stabilize a nucleophilic water molecule for an in-line attack of the γ-phosphate [17]. The position of the γ-phosphate is not changed in Rnd3 but two water molecules close to the γ-phosphate which are coordinated by Ser32, Ser79 and by the conserved Gly80, respectively, are in a different position compared to RhoA (Fig. 2B). The side chain of Ser32, on the other hand, would sterically interfere with the arginine finger of RhoGAP [8,24]. In conclusion, all requirements for a functional GTPase machinery are missing which suggests that Rnd3 exists only in the GTP-bound form and that Rnd proteins may not be regulated by the conventional cycling mechanism.

3.3. Surface areas

Signal transduction pathways are induced or inhibited through specific protein–protein interactions that often provide well defined interfaces concerning shape and electrostatic complementarity [25]. The solvent accessible surface area of

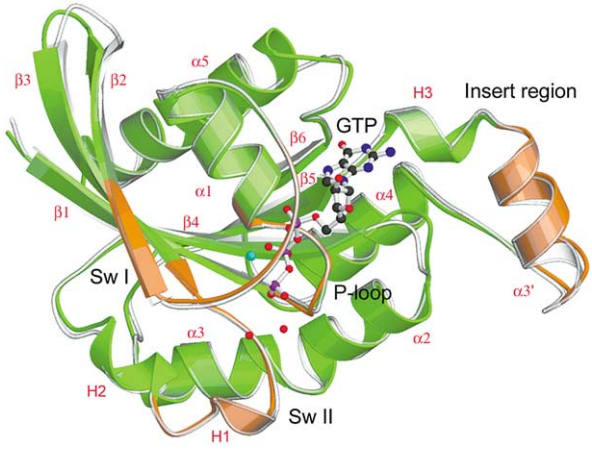

Fig. 1. Rnd3 Structure. Ribbon representation of Rnd3·GTP (green) compared with RhoA(G12V)·GTPγS (grey) [17] were analyzed by the program DSSP [40] and drawn using the program Bobscript [41,42]. Structural comparison of Rnd3 and RhoA was carried out with the least squares option of the program O [18]. P-loop, switch I, switch II and insert-helix are highlighted in orange.

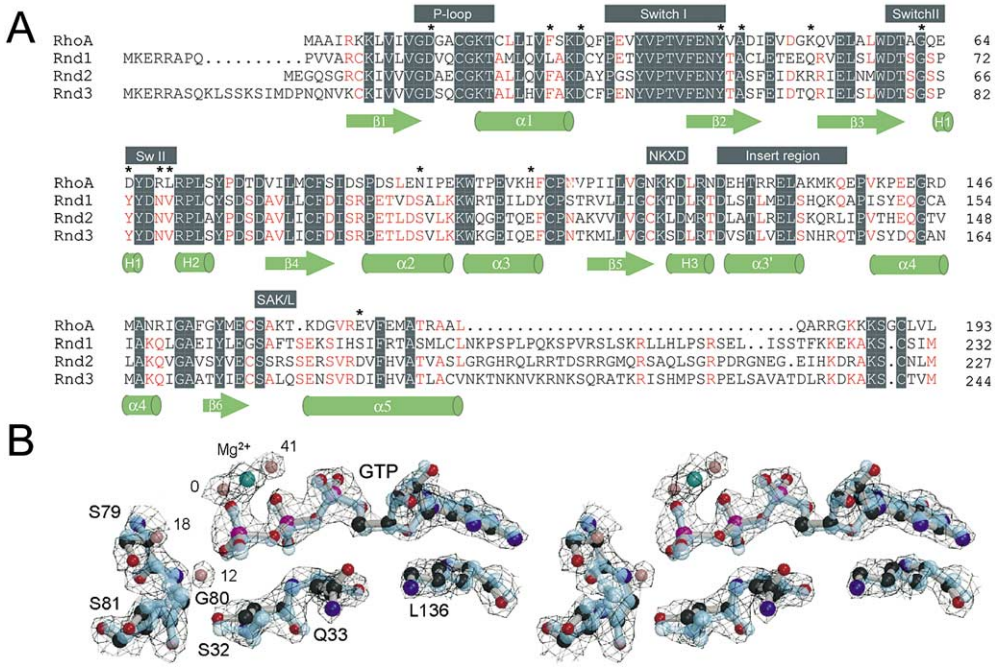

Fig. 2. Rnd proteins and GTP-binding. A: Sequence alignment of the Rnd proteins was performed using the program GeneDoc [44]. Invariant amino acids are boxed and identical residues in three proteins are red. Structural motives characteristic for small GTPases are indicated by dark boxes: P-loop, switch I, switch II and Rho-insert region. The assignment for Rnd3 is based on the final refined model (Table 1). Amino acids marked by asterisks indicate special residues discussed in the text. B: GTPase-deficient center. Stereo-view of the final $2F_o-F_c$ omit electron density map around the nucleotide-binding site of Rnd3 and RhoA (blue) drawn with Bobscript [42]. The map was calculated with the final refined atomic model by simulated annealing after the removal of the Mg^{2+} ion and the GTP. The Rnd3 residues and water molecules (orange) are highlighted.

both Rnd3 and RhoA structures exhibits major differences which are mainly due to low sequence homology (43% identity for the G-domain, Figs. 2A and 3A). Rnd3 shows a higher density of non-polar residues most notably at the regions of the β2–β3-strands, the insert- and α5-helices. The β2-strand of Rnd3, for instance, forms a hydrophobic groove which is flanked by alternating positive and negative charges. Interestingly, the switch regions show only minor changes concerning the shape (Fig. 3A) and nearly no differences concerning the electrostatic potentials (not shown).

3.4. Interacting interfaces

The proposed Rnd3 antagonism with RhoA for common interacting partners presumes that Rnd3 reproduces essential structural features of RhoA to bind and sequester RhoA regulators or effectors. In order to prove such a structural mimicry we analyzed the interfaces of RhoA interacting with ADP-ribosylation enzymes, GDIs, GAPs, GEFs and effectors, and compared them with the corresponding surface areas of Rnd3 (Fig. 3B).

3.4.1. ADP-ribosylation. The biological activities of Rho GTPases can be blocked by C3-like transferases from *Clostridium botulinum* ($C3^{Bot}$), which ADP-ribosylate RhoA (at Asn41), but not Rnd3 [26]. A novel C3-like exoenzyme from *Staphylococcus aureus* ($C3^{Stau}$) has been reported to modify efficiently RhoA at Asn41 and with a slower velocity also Rnd3 at the corresponding Asn59 [27]. From the structural and biochemical data, a hydrophobic patch on the surface of RhoA formed by Val38, Phe39, Val43, Trp58 and Leu72 has been proposed to bind the C3 exoenzymes (Fig. 3B) [26,28,29]. Thr61 and Ser74 in Rnd3 that are different compared to Val43 and Ala56 (which is close to the patch) in RhoA, may affect the interaction between the C3-transferase and Rnd3. Furthermore, the side chains of the asparagines 59 and 41 of Rnd3 and RhoA exhibit a different orientation (Fig. 3B). Unlike RhoA where Asn41 is exposed to the solvent, Asn59 in Rnd3 is locked in a more restricted and less accessible conformation due to its interaction with Ser74 (Ala56 in RhoA; Fig. 3B). Thus, we propose that both the divergence in the hydrophobic patch and the different coordination of Asn59 may cause the different modification rates.

3.4.2. RhoGDI-binding. From four different crystal structures it is known that GDI-binding utilizes the switch I/II, the adjacent α3-helix and the geranylgeranyl moiety [30–33]. The GDI-domain interacting interface of RhoA is predominantly conserved in Rnd3 except for Asn86 and Glu123 (Arg68 and His105 in RhoA; Fig. 3B). The particular role of Arg68 and His105 is to bind the C-terminal domain of GDI and stabilize its interaction with the N-terminal GDI-domain. The C-terminal domain subsequently binds to the geranylgeranyl moiety of the Rho proteins leading to membrane release [31,32]. We propose that the N-terminal regulatory domain of RhoGDI may bind to Rnd3 but any cellular GDI activity on Rnd3 remains unlikely because Asn86 and Glu123 in Rnd3 may electrostatically clash with the C-terminal domain of the GDI. In addition, it has been shown recently that RhoGDI indeed does not extract Rnd3 from the membrane [34].

3.4.3. RhoGAP-binding. As described above, the GTPase reaction of Rnd3 is resistant towards RhoGAP activation because of the absence of a catalytically competent glutamine (Ser81 in Rnd3) and the sterical clash of the arginine finger (RhoGAP) with Ser32 (Rnd3). It has been shown that the

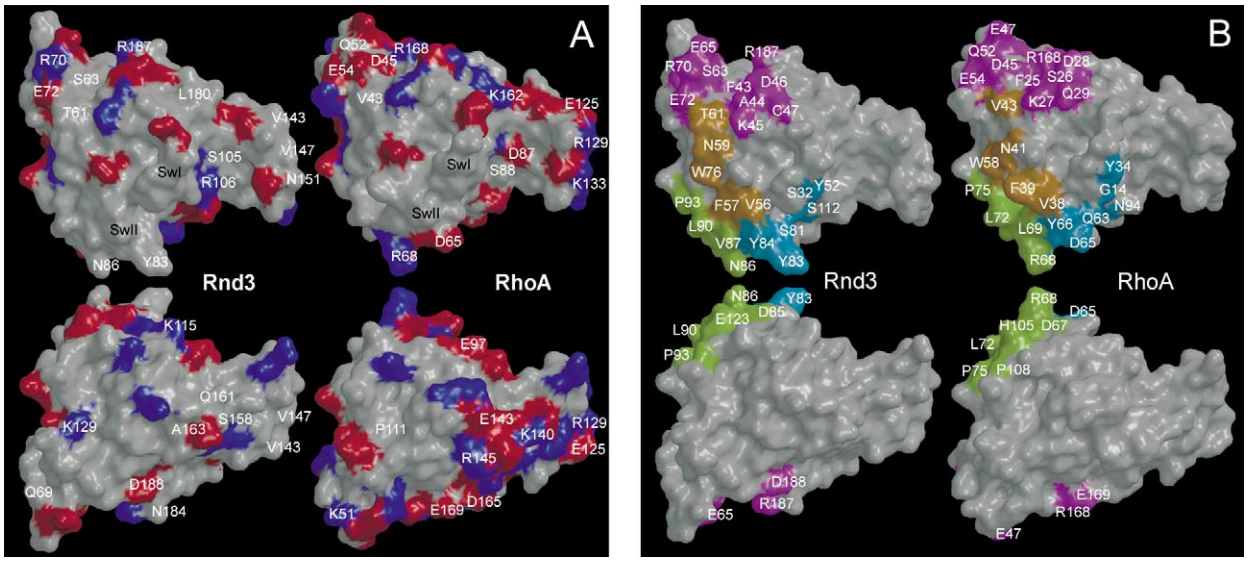

Fig. 3. Comparison of the surface and interacting areas of Rnd3 and RhoA. A: Surface deviations. Rnd3 (left panel) and RhoA (right panel) in the same orientation (upper panel) as in Fig. 1 and the back view (180° rotation around *x*-axis, lower panel) are presented as GRASP images [43]. Positively charged amino acids are blue, negatively charged amino acids are red. Surface residues deviating between Rnd3 and RhoA are marked (single letter code). B: Interacting interfaces of RhoA. Residues of RhoA involved in binding of RhoGDI (green), p50RhoGAP (blue), PKN (pink) and C3-transferases (orange) and the corresponding residues of Rnd3 are highlighted.

Gly12 (to Val) mutant of Ras still binds to RasGAP with similar affinity compared to wild-type but without subsequent stimulation of the GTPase reaction [35,36]. It is known that the RhoA–RhoGAP interaction is mediated through the switch regions and to a lower extent through the P-loop and α3-helix [24]. Four of the six residues of RhoA that are involved in an extensive hydrogen-bonding network with RhoGAP deviate in Rnd3 (Figs. 2A and 3B). Most interestingly, the corresponding residue to Asp65 of RhoA, which contacts Lys122 and Arg126 of RhoGAP and stabilize the RhoA switch II region, is Tyr83 in Rnd3. This may cause a sterical clash between Rnd3 and RhoGAP. These structural differences and the fact that the binding affinity of diverse RhoGAPs for RhoA is very low (between 2 and 90 μM) [37], make a Rnd3–RhoGAP interaction unlikely.

3.4.4. RhoGEF-binding. Since the Rnd proteins do not hydrolyze GTP and are resistant towards GAP activity, and since the physiological GTP concentration in the cell is 10-fold higher than that for GDP, we presume that these Rho-related proteins are not subjected to any GEF-mediated activation. However, it has also been suggested that the effect of Rnd proteins on Rho signalling might arise from their interference with the upstream signals leading to Rho activation [9]. Thus, we would like to address the question whether Rnd3 may bind and sequester RhoGEFs. Presently, no RhoA–RhoGEF structure is available but fortunately the structure of Cdc42 in complex with the DH/PH fragment of Dbs is known which also efficiently activates the nucleotide exchange reaction of RhoA [38]. The vast majority of Dbs-binding residues of the Cdc42 switch regions and α3-helix are not only conserved in RhoA but also in Rnd3. The only deviations are Arg68 and His105 which correspond to Asn86 and Glu123 in Rnd3, respectively (Fig. 3B). Interestingly, Arg66 and His103 of Cdc42 form a hydrogen-bonding network with the Dbs PH-domain [38]. Accordingly, we suggest that Rnd3 may bind the DH- but not the PH-domain as shown for the Cdc42·Dbs complex.

3.4.5. Effector binding. The most fundamental protein–protein interaction in signal transduction is the specific and selective interaction of the GTP-binding proteins with various downstream effectors [3]. It is known from the crystal structure of RhoA–PKN that the N-terminus of PKN binds three regions of RhoA, the switch I, β2/β3-strands and α5-helix [39]. Eight of the 17 residues of RhoA interacting with PKN, are not conserved in Rnd3 (Figs. 1, 2 and 3B). This and the differences at the PKN-binding surface area argue against a Rnd3 interaction with PKN and PKN-related proteins Rhotekin and Rhophilin. Unfortunately, we cannot predict any Rnd3 interaction with ROCK and mDia since there is no structural data available. These effectors which are mediators of the Rho-induced formation of stress fiber and focal adhesion, however, would be the appropriate targets for the Rnd proteins concerning their antagonistic effects on RhoA.

4. Conclusions

Despite a high structural homology, the GTP structure of Rnd3 revealed significant differences compared to the GTPγS structure of RhoA. Both proteins show remarkable differences at certain surface areas responsible for the interaction of RhoA with its interacting partners. Conventional mechanisms (GDI, GAP and GEF) known for most small GTPases may not be utilized to regulate Rnd3 activity. A Rnd3 interaction with Rho effectors such as PKN, Rhophilin and Rhotekin is quite unlikely, but no statement regarding ROCK, mDia and Citron interaction with Rnd3 is possible, yet, because they are structurally poorly investigated. Rnd proteins are expressed in diverse tissues. Whereas Rnd3 is ubiquitously expressed at a low basic level, Rnd1 and Rnd2 are expressed in brain and testis, respectively [6]. This different expression pattern and the high sequence homology between the G-domains (almost 90%) support the notion that the Rnd proteins may recruit similar interacting partners. Important questions as how the cellular activities of the Rnd proteins are regulated and

whether they share common downstream targets with RhoA, however, remain to be answered.

Acknowledgements: We would like to thank Alfred Wittinghofer for constant support, Guido W. Swart for providing the cDNA of human Rnd3, Klaus Scheffzek and Oliver Daumke for critical reading of the manuscript, and Andreas Arndt for expert technical help. L.B. is supported by grants from the Deutsche Forschungsgemeinschaft (AH 92/1-1). D.B. is supported by the BMBF and the Fonds der Chemischen Industrie.

References

[1] Ridley, A.J. (2001) Trends Cell Biol. 11, 471–477.
[2] Vetter, I.R. and Wittinghofer, A. (2001) Science 294, 1299–1304.
[3] Bishop, A.L. and Hall, A. (2000) Biochem. J. 348, 241–255.
[4] Olofsson, B. (1999) Cell Signal. 11, 545–554.
[5] Chardin, P. (1999) Prog. Mol. Subcell. Biol. 22, 39–50.
[6] Foster, R., Hu, K.Q., Lu, Y., Nolan, K.M., Thissen, J. and Settleman, J. (1996) Mol. Cell Biol. 16, 2689–2699.
[7] Abrams, S.I., Hand, P.H., Tsang, K.Y. and Schlom, J. (1996) Semin. Oncol. 23, 118–134.
[8] Scheffzek, K., Ahmadian, M.R., Kabsch, W., Wiesmüller, L., Lautwein, A., Schmitz, F. and Wittinghofer, A. (1997) Science 277, 333–338.
[9] Nobes, C.D., Lauritzen, I., Mattei, M.G., Paris, S., Hall, A. and Chardin, P. (1998) J. Cell Biol. 141, 187–197.
[10] Guasch, R.M., Scambler, P., Jones, G.E. and Ridley, A.J. (1998) Mol. Cell Biol. 18, 4761–4771.
[11] Watanabe, N., Kato, T., Fujita, A., Ishizaki, T. and Narumiya, S. (1999) Nat. Cell Biol. 1, 136–143.
[12] Hansen, S.H., Zegers, M.M., Woodrow, M., Rodriguez-Viciana, P., Chardin, P., Mostov, K.E. and McMahon, M. (2000) Mol. Cell Biol. 20, 9364–9375.
[13] Wunnenberg-Stapleton, K., Blitz, I.L., Hashimoto, C. and Cho, K.W. (1999) Development 126, 5339–5351.
[14] Ahmadian, M.R., Zor, T., Vogt, D., Kabsch, W., Selinger, Z., Wittinghofer, A. and Scheffzek, K. (1999) Proc. Natl. Acad. Sci. USA 96, 7065–7070.
[15] Otwinowski, Z. and Minor, W. (1997) in: 'Methods in Enzymology', Vol. 276: Macromolecular Crystallography, Part A (Carter, C.W., Jr. and Sweet, R.M., Eds.), pp. 307–327, Academic Press.
[16] Navaza, J. (1994) Acta Crystallogr. A50, 157–163.
[17] Ihara, K., Muraguchi, S., Kato, M., Shimizu, T., Shirakawa, M., Kuroda, S., Kaibuchi, K. and Hakoshima, T.J. (1998) J. Biol. Chem. 273, 9656–9666.
[18] Jones, T.A., Zou, J.Y., Cowan, S.W. and Kjeldgaard, M. (1991) Acta Crystallogr. A47, 110–119.
[19] Brunger, A.T., Adams, P.D., Clore, G.M., DeLano, W.L., Gros, P., Grosse-Kunstleve, R.W., Jiang, J.S., Kuszewski, J., Nilges, N., Pannu, N.S., Read, R.J., Rice, L.M., Simonson, T. and Warren, G.L. (1998) Acta Crystallogr. D54, 905–921.
[20] Feltham, J.L., Dotsch, V., Raza, S., Manor, D., Cerione, R.A., Sutcliffe, M.J., Wagner, G. and Oswald, R.E. (1997) Biochemistry 36, 8755–8766.
[21] Rudolph, M.G., Wittinghofer, A. and Vetter, I.R. (1998) Protein Sci. 8, 778–787.
[22] Hirshberg, M., Stockley, R.W., Dodson, G. and Webb, M.R. (1997) Nat. Struct. Biol. 4, 147–152.
[23] Wei, Y., Zhang, Y., Derewenda, U., Liu, X., Minor, W., Nakamoto, R.K., Somlyo, A.V., Somlyo, A.P. and Derewenda, Z.S. (1997) Nat. Struct. Biol. 4, 699–703.
[24] Rittinger, K., Walker, P.A., Eccleston, J.F., Smerdon, S.J. and Gamblin, S.J. (1997) Nature 389, 758–762.
[25] Hu, Z., Ma, B., Wolfson, H. and Nussinov, R. (2000) Proteins 39, 331–342.
[26] Wilde, C. and Aktories, K. (2001) Toxicon 39, 1647–1660.
[27] Wilde, C., Chhatwal, G.S., Schmalzing, G., Aktories, K. and Just, I. (2001) J. Biol. Chem. 276, 9537–9542.
[28] Han, S., Arvai, A.S., Clancy, S.B. and Tainer, J.A. (2001) J. Mol. Biol. 305, 95–107.
[29] Wilde, C., Just, I. and Aktories, K. (2002) Biochemistry 41, 1539–1544.
[30] Longenecker, K., Read, P., Derewenda, U., Dauter, Z., Liu, X., Garrard, S., Walker, L., Somlyo, A.V., Nakamoto, R.K., Somlyo, A.P. and Derewenda, Z.S. (1999) Acta Crystallogr. D55, 1503–1515.
[31] Scheffzek, K., Stephan, I., Jensen, O.N., Illenberger, D. and Gierschik, P. (2000) Nat. Struct. Biol. 7, 122–126.
[32] Hoffman, G.R., Nassar, N. and Cerione, R.A. (2000) Cell 100, 345–356.
[33] Grizot, S., Faure, J., Fieschi, F., Vignais, P.V., Dagher, M.C. and Pebay-Peyroula, E. (2001) Biochemistry 40, 10007–10013.
[34] Forget, M.A., Desrosiers, R.R., Gingras, D. and Beliveau, R. (2002) Biochem. J. 361, 243–254.
[35] Gideon, P., John, J., Frech, M., Lautwein, A., Clark, R., Scheffler, J.E. and Wittinghofer, A. (1992) Mol. Cell Biol. 12, 2050–2056.
[36] Bollag, G. and McCormick, F. (1992) Nature 356, 663–664.
[37] Zhang, B. and Zheng, Y. (1998) Biochemistry 37, 5249–5257.
[38] Rossman, K.L., Worthylake, D.K., Snyder, J.T., Siderovski, D.P., Campbell, S.L. and Sondek, J. (2002) EMBO J. 21, 1315–1326.
[39] Maesaki, R., Shimizu, T., Ihara, K., Kuroda, S., Kaibuchi, K. and Hakoshima, T. (1999) J. Struct. Biol. 126, 166–170.
[40] Kabsch, W. and Sander, C. (1983) Biopolymers 22, 2577–2637.
[41] Kraulis, P.J. (1991) J. Appl. Crystallogr. 24, 946–950.
[42] Esnouf, R.M. (1997) J. Mol. Graph. 15, 133–138.
[43] Nicholls, A., Sharp, K.A. and Honig, B. (1991) Proteins 11, 281–296.
[44] Nicholas, K.B., Nicholas Jr., H.B. and Deerfield, D.W.I. (1997) EMBnet News 4, 14.